ISBN: 978-3-95450-231-8 ISSN: 2673-5490 doi: 10.18429/JACoW-IPAC2023-TUPL033

SPACE CHARGE EFFECTS ON DENSITY-MODULATED ELECTRON BEAMS IN DRIFT SPACES

S. Khan*†, Center for Synchrotron Radiation, TU Dortmund University, Dortmund, Germany
G. Perosa[1], F. Sottocorona[1], E. Allaria, A. Brynes, G. Penco, P. R. Ribič, S. Spampinati, C. Spezzani, M. Trovò, L. Giannessi[2], G. De Ninno[3], Elettra-Sincrotrone Trieste SCpA, Basovizza, Italy
E. Ferrari, E. Schneidmiller, Deutsches Elektronen-Synchrotron DESY, Hamburg, Germany
[1] also at Università degli Studi di Trieste, Trieste, Italy
[2] also at Laboratori Nazionali di Frascati, INFN, Frascati, Italy
[3] also at University of Nova Gorica, Nova Gorica, Slovenia

Abstract

Seeding of free-electron lasers (FELs) is based on a periodic modulation of the electron energy by an external radiation pulse converted to a density modulation in a dispersive section. In complex configurations such as cascaded high-gain harmonic generation (HGHG) or echo-enabled harmonic generation (EEHG), the density-modulated electron beam may need to be propagated through drift spaces or detuned undulators before starting the lasing process in the FEL undulators. In such a case, space charge tends to smear out the maxima of the electron density but also reduces the energy spread of the electrons between them. Studies of the evolution of the density-modulated beam in drift spaces and detuned undulators were carried out in different configurations of the FEL-1 beamline of FERMI, the FEL user facility at Elettra Sincrotrone Trieste in Italy.

INTRODUCTION

The FERMI user facility [1] at the Elettra laboratory located near Trieste, Italy, provides powerful radiation in the spectral range from 100 to 4 nm with two free-electron laser (FEL) lines, FEL-1 and FEL-2. Both rely on the use of an external seed laser to initiate the process of FEL amplification and coherent emission in order to provide a high degree of longitudinal and transverse coherence, enabling experiments not possible with other radiation sources. Currently, FEL-1 [2] is based on high-gain harmonic generation (HGHG) [3, 4] with a single undulator (modulator) for seeding, a dispersive section to convert the laser-induced energy modulation into a density modulation, and six undulators (radiators) for the FEL process – see Fig. 1. In order to extend its spectral range, FEL-1 is presently being upgraded to implement the echo-enabled harmonic generation (EEHG) [5–7] scheme, employing two modulators and two dispersive sections to generate a longitudinal density distribution with higher harmonic content [8]. FEL-2 [9], on the other hand, is based on two successive modulator-radiator stages employing a fresh-bunch scheme (HGHG-FB) [10].

In an externally seeded FEL, the transformation of the energy modulation into a density modulation by a dispersive section gives rise to longitudinal space charge (LSC) effects.

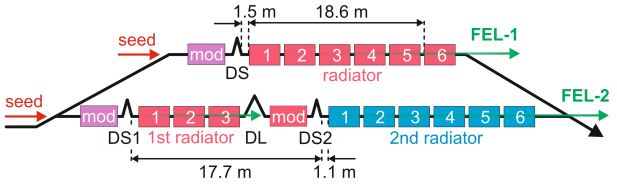

Figure 1: Schematic view of the seeded FEL lines of FERMI as of summer 2022 with modulators (mod), radiators, dispersive sections (DS), and a delay line (DL) for two-staged HGHG (figure not to scale, see also Table 1).

If the radiator is placed immediately after the dispersive section, the FEL process starts before LSC effects become significant. On the other hand, the recent advent of more complex seeding schemes, such as HGHG-FB and EEHG mentioned above, may require the density-modulated electrons to be transported through drift sections before entering the radiator. Studies at FEL-2 with energy modulation in the first modulator and using either the first or second dispersive section (DS1 and DS2 in Fig. 1) showed a strong degradation of the density-modulated beam when it was transported over 18.8 m (using DS1) instead of only 1.1 m (using DS2). The energy of the FEL pulse from the second radiator was reduced by a factor of four [11]. Recent results from the remodeled FEL-1 line confirm that the HGHG output is not influenced when the energy-modulated beam is transported over a longer distance before the dispersive section.

After discussing the one-dimensional theory of beam dynamics under the influence of LSC, this paper shows results of experiments conducted in 2022 at FEL-1, where the distance between the dispersive section (DS) and a subsequent single radiator module (1 to 6) was varied to study the LSC effect as a function of the drift length.

THEORY AND SIMULATION

A laser-induced sinusoidal modulation of the electron energy followed by a dispersive section with an appropriate R_{56} value leads to sharp maxima of the longitudinal electron density spaced at the laser wavelength λ_L. Given a tilted sinusoidal phase space distribution, electrons preceding a density maximum have a negative, trailing electrons a positive energy offset. As shown in Fig. 2, the repulsive LSC forces of the density maxima reduce the energy offset of elec-

* shaukat.khan@tu-dortmund.de
† Work supported by Heinrich-Hertz-Stiftung, MKW NRW, Düsseldorf.

ISBN: 978-3-95450-231-8 ISSN: 2673-5490 doi: 10.18429/JACoW-IPAC2023-TUPL033

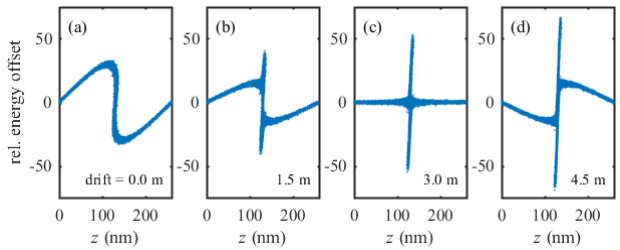

Figure 2: (a): Density-modulated electrons in longitudinal phase space along one seed wavelength. (b) to (d): LSC-induced evolution after drift lengths of 1.5 to 4.5 m.

trons between them, but the energy spread within the density maxima increases. While the increased energy spread leads to debunching, a previous simulation study [12] suggested that the flat energy distribution between the maxima may improve the output of HGHG at high harmonics because a larger fraction of the electrons is within the FEL bandwidth.

A one-dimensional model already provides good insight into the process. Following the notation of [12], the coupled equations in longitudinal phase space

$$\frac{dp_i}{d\tau} = \frac{2}{\alpha}\sum_{h=1}^{\infty} b_h \frac{\sin h\theta_i}{h} \quad \text{and} \quad \frac{d\theta_i}{d\tau} = \alpha\, p_i \qquad (1)$$

are iterated for macroparticles ($i = 1, \ldots n$) in small steps of plasma phase advance τ, which translates into position s in the laboratory frame via $\tau = k_\mathrm{P}\, s$, where $k_\mathrm{P} = \sqrt{e^2 n_0/m_\mathrm{e} c^2 \varepsilon_0 \gamma^3}$ is the plasma wavenumber [13] with the electron charge $-e$ and mass m_e, the electron density n_0, the dielectric constant ε_0, and the Lorentz factor γ. One phase space coordinate is the relative energy offset $p_i(\tau) = \eta_i/\sigma_\eta$ normalized to the relative energy spread σ_η with $\eta_i \equiv \Delta\gamma_i/\gamma$, the other is the phase $\theta_i = k_\mathrm{L} z_i = 2\pi z_i/\lambda_\mathrm{L}$ with the longitudinal coordinate z_i in a co-moving frame. Furthermore, $b_h = (1/n)\sum_i \exp(ih\theta_i)$ is the bunching factor at laser harmonic h, which is updated at every iteration, and the parameter $\alpha \equiv (k_\mathrm{L}/k_\mathrm{P})\,\sigma_\eta/\gamma^2$ normalizes the frequency of the plasma oscillaton given by Eq. (1).

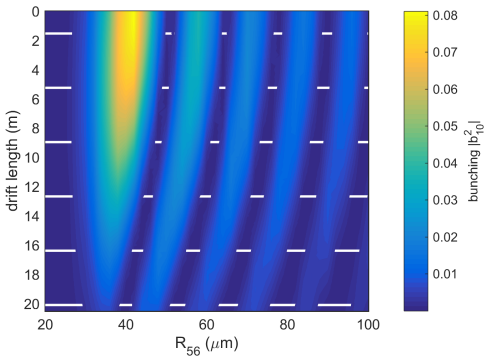

Figure 3: Squared bunching factor of the 10th seed harmonic as function of R_{56} and drift length. The white lines correspond to the drift between dispersive section and the undulators of the FEL-1 radiator. See text for further details.

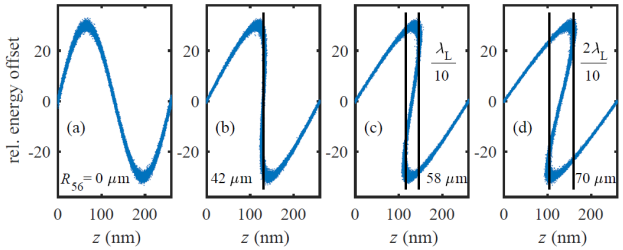

Figure 4: (a): Energy-modulated electrons in longitudinal phase space along one seed wavelength. (b) to (d): Density modulation with different R_{56} value of the dispersive section (vertical lines show the positions of density maxima).

The first of the coupled equations describes the change of energy due to a longitudinal electric field caused by a gradient of the charge distribution. The second equation can be rewritten as $dz_i/ds = \eta_i/\gamma^2$ meaning that relativistic particles with an energy offset change their longitudinal position due to a velocity mismatch.

Figure 3 shows an example of the squared bunching factor $|b_{10}|^2$ as function of R_{56} and drift length for a moderate peak current of 700 A (before density modulation). Along the R_{56} axis, the first maximum occurs for optimum density modulation. The nth maximum results from a modulation with two density maxima which are $(n-1)\lambda_\mathrm{L}/10$ apart as illustrated by Fig. 4 for $n \leq 3$. The bunching factor decreases strongly over a drift length of 20 m, but the LSC-induced reduction is different for each maximum, causing their relative height to change. Furthermore, the maxima are slightly shifted to lower R_{56} with increasing drift length because the LSC effect causes additional longitudinal dispersion.

In complex seeding setups, density-modulated electron beams may also be transported through undulators with detuned K parameters. Since an electron lags behind a photon by $\lambda_\mathrm{U}\left(1 + K^2/2\right)/2\gamma^2$ per undulator period λ_U [14], its motion can be described by a *reduced* Lorentz factor $\gamma_\mathrm{r} \equiv \gamma/\sqrt{1 + K^2/2}$. Thus, detuned undulators act like drift spaces in which the propagation of the electrons is retarded and the characteristic length for LSC-related effects is shortened. Both, drift spaces and detuned undulators, were studied experimentally as described next.

EXPERIMENTAL RESULTS

The layout of FERMI shown in Fig. 1 allows to study the evolution of the electron beam under variation of the drift length between dispersive section and radiator.

In one set of experiments, a single undulator of the FEL-1 radiator line was tuned to the 10th harmonic of the seed wavelength ($\lambda = 260$ nm) and was preceded by zero to five undulators with open magnetic gap acting as a variable drift space. The FEL pulse intensity was recorded using an intensity monitor ($\mathrm{I_0M}$) based on the photo-ionization of a low-density rare gas [15]. Using a grating spectrometer (PRESTO [16]) was not possible because the single-undulator signal was too low for this device. The measurements were performed

ISBN: 978-3-95450-231-8 ISSN: 2673-5490 doi: 10.18429/JACoW-IPAC2023-TUPL033

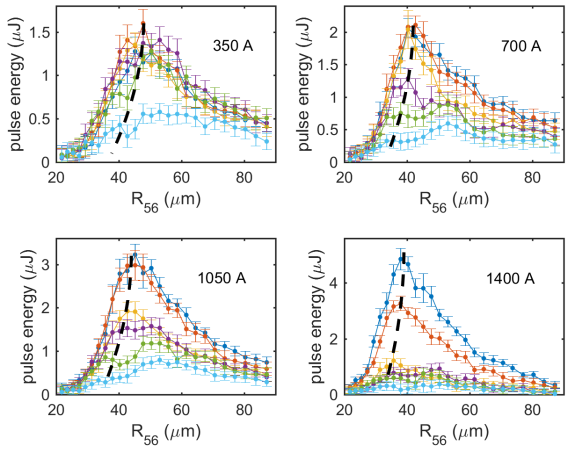

Figure 5: Measured single-undulator pulse energy as function of R_{56} for drift lengths from 1.5 to 20.1 m (sequence: blue, red, orange, purple, green, cyan) and peak currents from 350 to 1400 A. The dashed lines indicate the shift of the first maximum towards lower R_{56}.

under variation of the strength R_{56} of the dispersive section. Data were recorded for different values of electron density tuned by the magnetic bunch compressor BC1. Table 1 summarizes the experimental parameters.

Using a single undulator of length 2.4 m as radiator, the effect of FEL dynamics is small and the pulse energies can be assumed to correspond to the squared bunching factors from the simulation. Figure 5 shows the pulse energy of the 10th harmonic of the seed while scanning the R_{56} value of the dispersive section. Background radiation from the dispersive section magnets, which shows up with a characteristic R_{56}-dependence in the I_0M monitor, was subtracted. The scans were performed for six values of drift length (color code given in the figure caption) and four compressor settings with the estimated peak current given in each panel.

The nearly Gaussian intensity distribution along the seed pulse leads to a variation of the energy modulation amplitude and thus to a spread of R_{56} values for optimum bunching. Therefore, the peak structure shown in the simulation with uniform energy modulation is strongly washed out but still recognizable in the R_{56} scans. The effect of debunching, i.e.,

Table 1: Summary of Experimental Parameters

Parameter	Value
beam energy E	1300 MeV
relative energy spread σ_η	$4 \cdot 10^{-5}$
peak current I	350 to 1400 A
normalized emittance $\varepsilon_{x,y}$	$1 \cdot 10^{-6}$ m rad
average beta function $\beta_{x,y}$	10 m
seed wavelength λ_L	230 to 260 nm
seed pulse energy E_L	15 to 25 μJ
longitudinal dispersion R_{56}	0 to 100 μm
drift length s	1.5 to 20.1 m (6 steps)

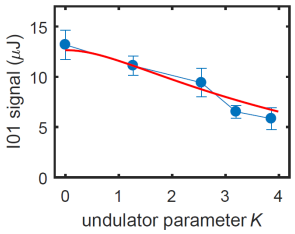

Figure 6: Measured pulse energy in radiator 3 of FEL-1 (see Fig. 1) as function of the K parameter of the preceding detuned undulators. The red line depends on the reduced Lorentz factor γ_r decreasing with increasing K (see text).

the reduction of pulse energy with increasing drift length, is stronger for higher peak current, confirming its collective nature. The dashed lines in Fig. 5 indicate the tendency of the maxima to shift towards lower R_{56} with increasing drift length as in the simulation. The debunching effect on the first maximum is stronger than on the subsequent peaks, which causes the centroid of the distribution to shift towards higher R_{56} values.

In another experiment, a single undulator of the FEL-1 radiator line was tuned to the 6th seed harmonic and was preceded by detuned undulators. Figure 6 shows the case of two undulators under variation of their K value. The red line is proportional to $\exp(-2d_U/\gamma_r - d/\gamma)$, where γ_r is the reduced Lorentz factor along each undulator of length d_U while d is the combined length of the in-between drift spaces. The measured intensity reduces with increasing K value as expected.

CONCLUSIONS

For density-modulated electron beams in seeded FELs, the peak current is high enough to cause LSC-induced debuncing over a few meters in a drift section. Measurements at FERMI under variation of drift length, longitudinal dispersion, and electron density are in good qualitative agreement with a simple one-dimensional model. Generally, long drift spaces between dispersive section and radiator should be avoided in the design of FELs with complex seeding schemes whereas the propagation of an unbunched beam is not critical. Except for high electron density (peak current 1400 A), the signals for the first two drift lengths (1.5 m and 5.2 m) in Fig. 5 seem to be comparable, which may indicate an enhanced FEL amplification due to reduced energy spread as suggested in [12]. Definitive conclusions, however, may require further measurements.

ACKNOWLEDGEMENTS

S.K. would like to thank the TU Dortmund University and its Physics Department for granting a sabbatical, which was supported by the Heinrich-Hertz-Stiftung NRW. The kind hospitality of the FERMI team and the support during the measurements and data analysis is gratefully acknowledged.

ISBN: 978-3-95450-231-8 ISSN: 2673-5490 doi: 10.18429/JACoW-IPAC2023-TUPL033

REFERENCES

[1] E. Allaria *et al.*, "The FERMI free-electron laser", *J. Synchrotron Radiat.*, vol. 22, pp. 485-491, 2015. doi:10.1107/S1600577515005366

[2] E. Allaria *et al.*, "Highly coherent and stable pulses from the FERMI seeded free-electron laser in the extreme ultraviolet", *Nat. Photonics*, vol. 6, pp. 699-704, 2012. doi:10.1038/nphoton.2012.233

[3] I. Boscolo, V. Stagno, "The converter and the transverse optical klystron", *Nuovo Cimento B*, vol. 58, pp. 267-285, 1980. doi:10.1007/BF02874012

[4] L. H. Yu, "Generation of intense uv radiation by subharmonically seeded single-pass free-electron lasers", *Phys. Rev. A*, vol. 44, pp. 5178-5193, 1991. doi:10.1103/PhysRevA.44.5178

[5] G. Stupakov, "Using the beam-echo effect for generation of short-wavelength radiation", *Phys. Rev. Lett.*, vol. 102, p. 74801, 2009. doi:10.1103/PhysRevLett.102.074801

[6] D. Xiang and G. Stupakov, "Echo-enabled harmonic generation free electron laser", *Phys. Rev. Spec. Top. Accel. Beams*, vol. 12, p. 030702, 2009. doi:10.1103/PhysRevSTAB.12.030702

[7] P. Rebernik Ribic *et al.*, "Coherent soft X-ray pulses from an echo-enabled harmonic generation free-electron laser", *Nat. Photonics*, vol. 13, pp. 555-561, 2019. doi:10.1038/s41566-019-0427-1

[8] C. Spezzani *et al.*, "FERMI upgrade to echo-enabled harmonic generation", presented at 14th Int. Particle Accelerator Conf. (IPAC'23), Venice, Italy, May 2023, paper TUPL035, this conference.

[9] E. Allaria *et al.*, "Two-stage seeded soft-X-ray free-electron laser", *Nat. Photonics*, vol. 7, pp. 913-918, 2013. doi:10.1038/nphoton.2013.277

[10] L.-H. Yu, I. Ben-Zvi, "High-gain harmonic generation of soft X-rays with the "fresh bunch" technique", *Nucl. Instrum. Methods Phys. Res., Sect. A*, vol. 393, pp. 96-99, 1997. doi:10.1016/S0168-9002(97)00435-X

[11] S. Khan *et al.*, "Evolution of microbunching in drift sections", presented at the 40th Int. Free-Electron Laser Conf. (FEL'22), Trieste, Italy, Aug. 2022, paper MOP01, to be published in the proceedings.

[12] E. Hemsing *et al.*, "Correlated Energy-Spread Removal with Space Charge for High-Harmonic Generation", *Phys. Rev. Letters*, vol. 113, p. 134802, 2014. doi:10.1103/PhysRevLett.113.134802

[13] J. Rosenzweig *et al.*, "Space-charge oscillations in a self-modulated electron beam in multi-undulator free-electron lasers", *Nucl. Instrum. Methods Phys. Res., Sect. A*, vol. 393, pp. 376-379, 1997. doi:10.1016/S0168-9002(97)00516-0

[14] H. Wiedemann, *Particle Accelerator Physics, Fourth Edition*, Cham, Switzerland: Springer, 2015.

[15] M. Zangrando *et al.*, "The photon analysis, delivery, and reduction system at the FERMI@Elettra free electron laser user facility", *Rev. Sci. Instrum.*, vol. 80, p. 113110, 2009. doi:10.1063/1.3262502

[16] C. Svetina *et al.*, "PRESTO, the on-line photon energy spectrometer at FERMI: design, features and commissioning results", *J. Synchrotron Rad.*, vol. 23, pp. 35-42, 2016. doi:10.1107/S1600577515021116